Statistical Analysis of Convective Updrafts in Tropical Cyclone Rainbands Observed by Airborne Doppler Radar

Nicholas R. Barron, Anthony C. Didlake Jr., Paul D. Reasor

(2022, *Journal of Geophysical Research*)

Introduction

- Tropical cyclone (TC) rainbands contain convective and stratiform features that can involve interactions with the BL, eyewall, and environment. The interactions can lead to large impacts on TC evolutions:

1. Rainbands can enlarge PV that spirals into the core and cause TCs to strengthen. (Franklin et al., 2006; May and Holland, 1999)
2. Rainband downdrafts by precipitation and compensating subsidence can reduce the BL θ_e air feeding into the eyewall. (e.g., Alland et al., 2021a; etc.)
3. Diabatic heating in rainbands can produce a local pressure minimum, which reduces the inflow to the eyewall. (Powell, 1990a; Wang, 2009)
4. Rainband can accelerate the local tangential wind and cause the expandsion of the wind field and SEF. (e.g., Bell et al., 2012; etc.)

Introduction

- The presence of sufficient environmental vertical wind shear (VWS) can let the rainbain turn into a broad, organized, asymmetric stationary band complex (SBC).
-

(Willoughby et al., 1984)

- SBC in DR and UR:
  - Low-level inflow -> intense updraft -> outflow in mid-levels (5-8 km)
  - Local tangential wind jets through stretching and tilting.
  - Downdraft at z = 2-4 km by precipitation drag
  - Downdraft at z = 6-8 km at the inner edge of rainband

(Barnes et al., 1983; Hence and Houze, 2008; Powell, 1990a, 1990b; Samsury and Zipser, 1995; Didlake and Houze, 2009)

- SBC in UL and DL:
  - A broad stratiform precipitation
  - Mesoscale descending inflow (MDI), which extends to BL, forced by midlevel latent cooling
  - New convection by cold pool form by MDI

(Didlake and Houze, 2013b; Didlake et al., 2018; Yu and Didlake, 2019; Yu et al., 2021; Li and Dai, 2020)

Introduction

- Rainband convection varies with radius.
  - Convective updrafts at smaller radii have a shallower vertical extent than those at larger radii due to lower CAPE and stronger filamentation at smaller radii.
  - Distant rainbands are buoyancy-driven and propagate with a locally generated cold pool.

(Bogner et al., 2000; Li and Fang, 2019; Molinari et al., 2013; Moon and Nolan, 2015; Tang et al., 2014)

- Limitations of the previous studies:
  - The simulations of case studies did not capture the variety of rainband features that occur in nature. (e.g., Barnes and Stossmeister, 1986; etc.)
  - Azimuthal average was usually used in the analyses. It obscures smaller-scale features important for TC evolution. (e.g., Reasor et al., 2013)
  - Some TC studies capture the convective-scale features across a few TC cases.

Introduction

- The goal of this study:
  - Understand the overall role of rainbands on TC evolution.
  - Understand the different rainband structures and processes that can occur.
  - Better understand the variety of rainband updraft structures along TC ($\geq 33\ m/s$).
  - Explore the detailed structure of the observed rainband convection.

- This study analyzes the convective-scale structure of TC rainbands by 10 years of airborne Doppler radar observations from Atlantic and central Pacific basin hurricanes.

- This study identifies the strongest rainband updrafts in each storm and focuses on their updrafts, convective-scale kinematic, and reflectivity structures by statistical analyses.

Data and Method

Airborne radar observations

- NOAA WP-3D Tail Doppler radar (TDR)
  - X-band
  - The beam oriented 20^o fore and aft
  - 3D wind fields were retrieved by the Doppler wind
  - Cartesian grid with dx = 2 km and dz = 0.5 km
  - 59 missions across 12 hurricane-strength TCs
  - From 2010 to 2019

- The 6-hr maximum wind speeds were from NOAA NHC HURDAT2 dataset.
- The storm centers were determined by TDR data.
- The TDR data were interpolated to the grid size of $(dz, d\theta, dr) = (0.5km, 2°, 2km)$.
- The storm-relative wind field were used in all analyses.
- To account for varying storm size, the radial is normalized by the RMW of each mission.

Data and Method

Updraft selection and updraft properties

- Automated updraft selection algorithm
    1. Define the updraft threshold: 95th % of w at 2-km height and 1.5 RMW.
    2. Define the convective updraft: clustering all connected data grids where w > above threshold
    3. The convective updrafts must be larger than 2 km at least one direction.
    4. Perform convective-stratiform classification algorithm on reflectivity. Only convective updraft with over 40% of convective region were selected.

storm track (Hurricane Research Division Best Track)
shear (NCEP Reanalysis-2; background 0~800 avg)

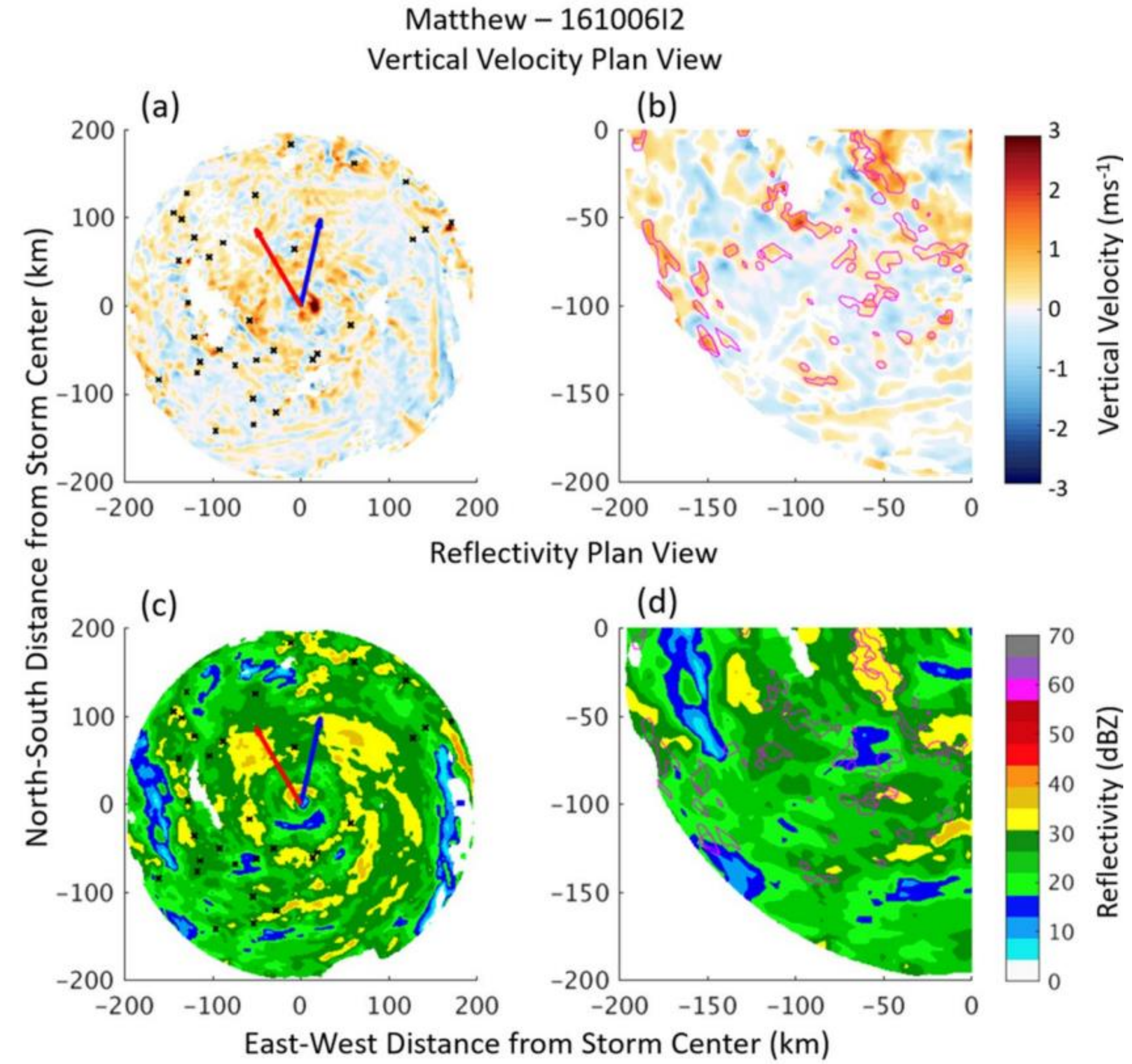

Data and Method

Updraft selection and updraft properties

storm track (Hurricane Research Division Best Track)
shear (NCEP Reanalysis-2; background 0~800 avg)

- Characteristic to be analyzed:
  - Normalized radius (r^*)
  - Shear-relative azimuthal (θ_s)
  - Track-relative azimuthal (θ_t)
  - Updraft base altitude
  - Updraft top altitude
  - Updraft depth
  - Updraft strength ($\max(w)$)

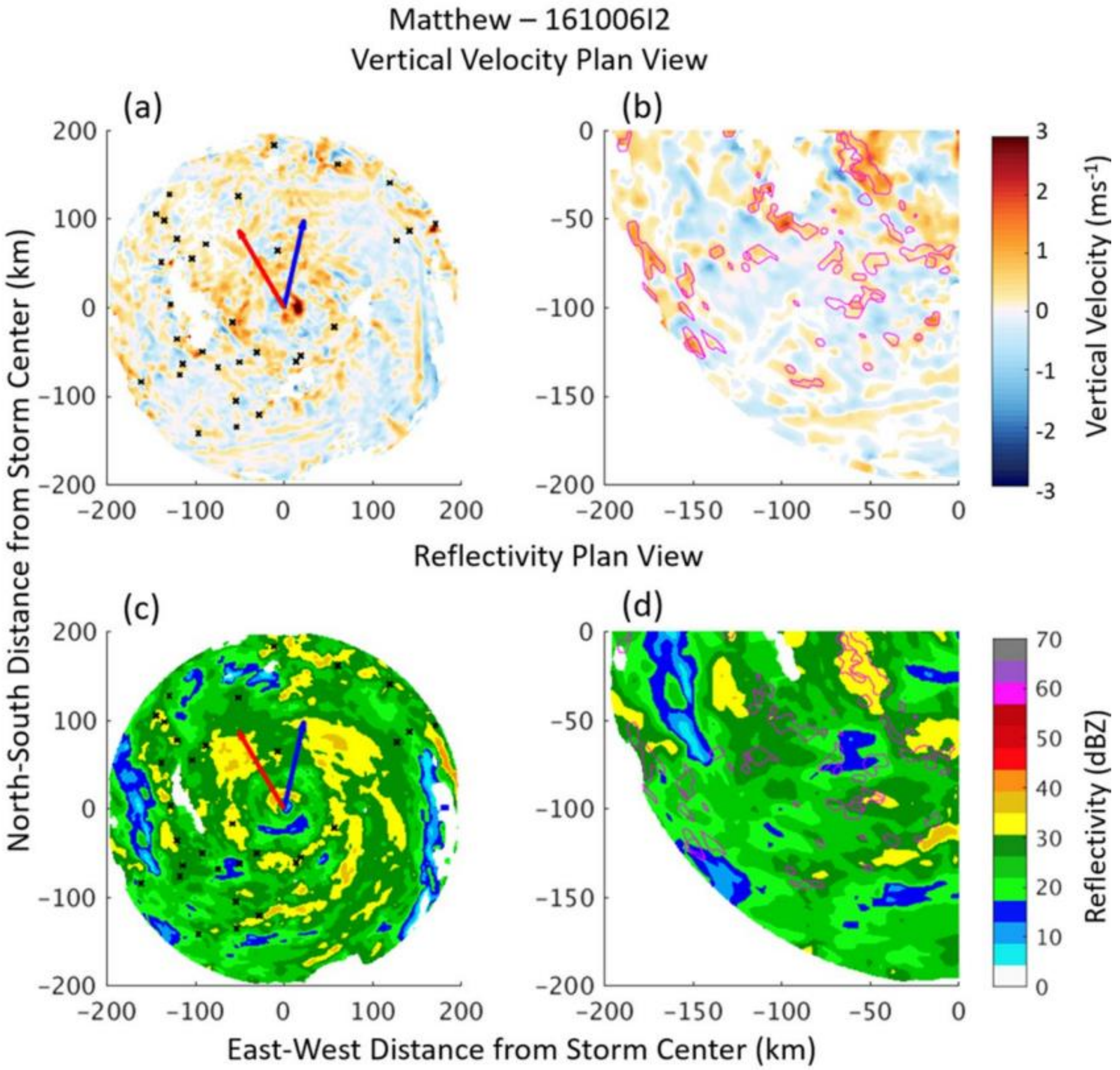

Analyses in an axisymmetric framework

Updraft size, strength, and location

- The frequency of updrafts decreases with increasing radius.
- A peaked distribution of base altitude is present at 2–4 RMW, and the distribution flattens at larger radii.
- Top altitude are largely above 6 km.
- Depth increases with increasing radius.
- Strength mainly distributes at 1-2 m/s. The relative frequency of 2-3 m/s at 4-6 RMW increases.

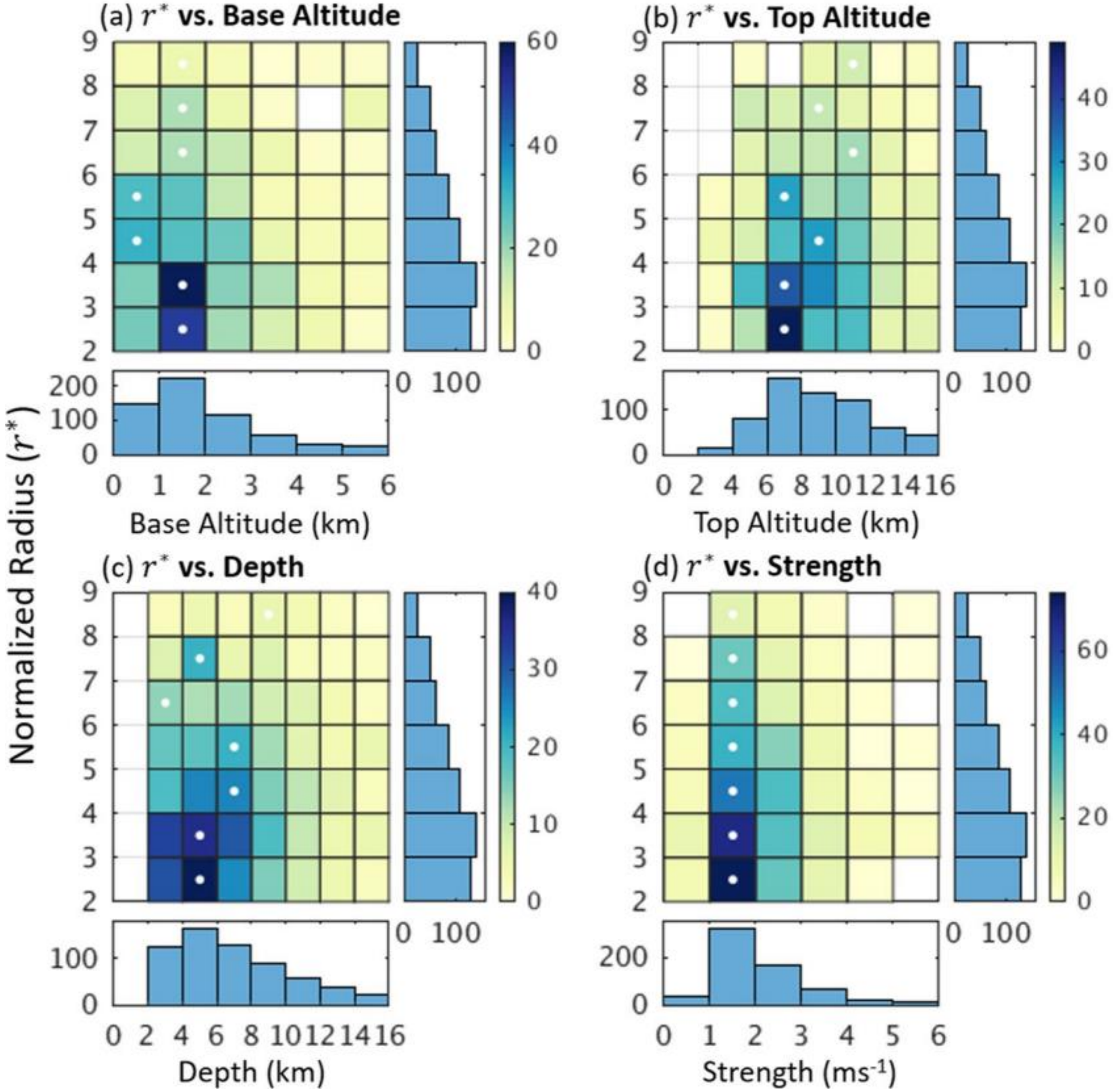

Analyses in an asymmetric framework

Updraft size, strength, and location

- Downshear side had more updraft, especially at DR.
- The updraft distributions in DL, UL, DR are more concentrated in shear > 4 m/s missions than those in all missions.
- Less organization in the right-of-track quadrants in missions with high track motions.

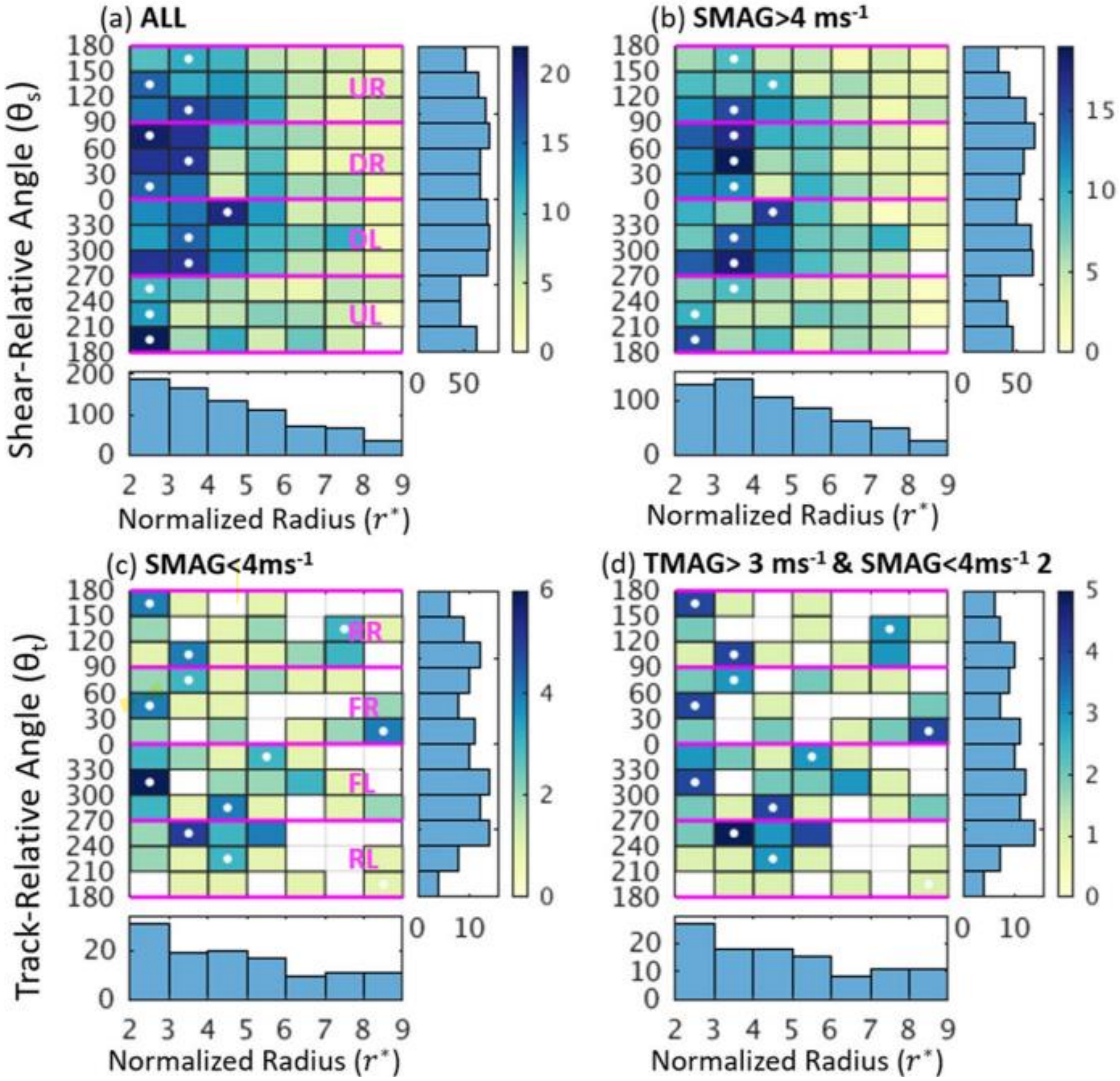

Analyses in an asymmetric framework

Updraft size, strength, and location

- The mean base altitude at downshear is highest.
- The mean top altitudes and mean depth at downshear quadrants are higher than those in upshear quadrants.

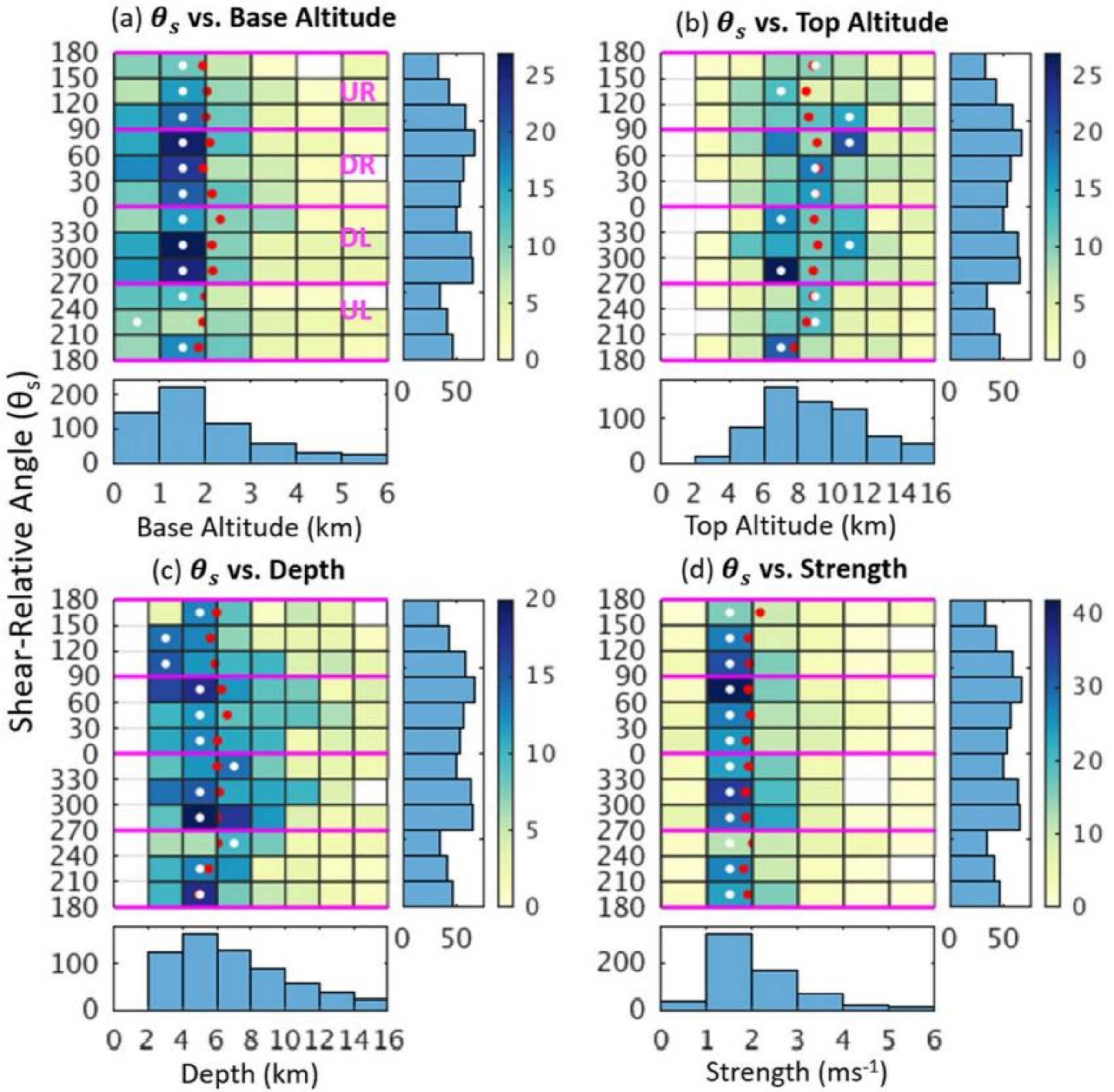

Total kinematics of updraft elements

Quadrant-averaged composites

Radial cross sections

- Normalized w
- u and w
- Reflectivity

Color: v’

$$v' = v - \bar{v}^{\pm 45^\circ}$$

It removes the WN2 signals.

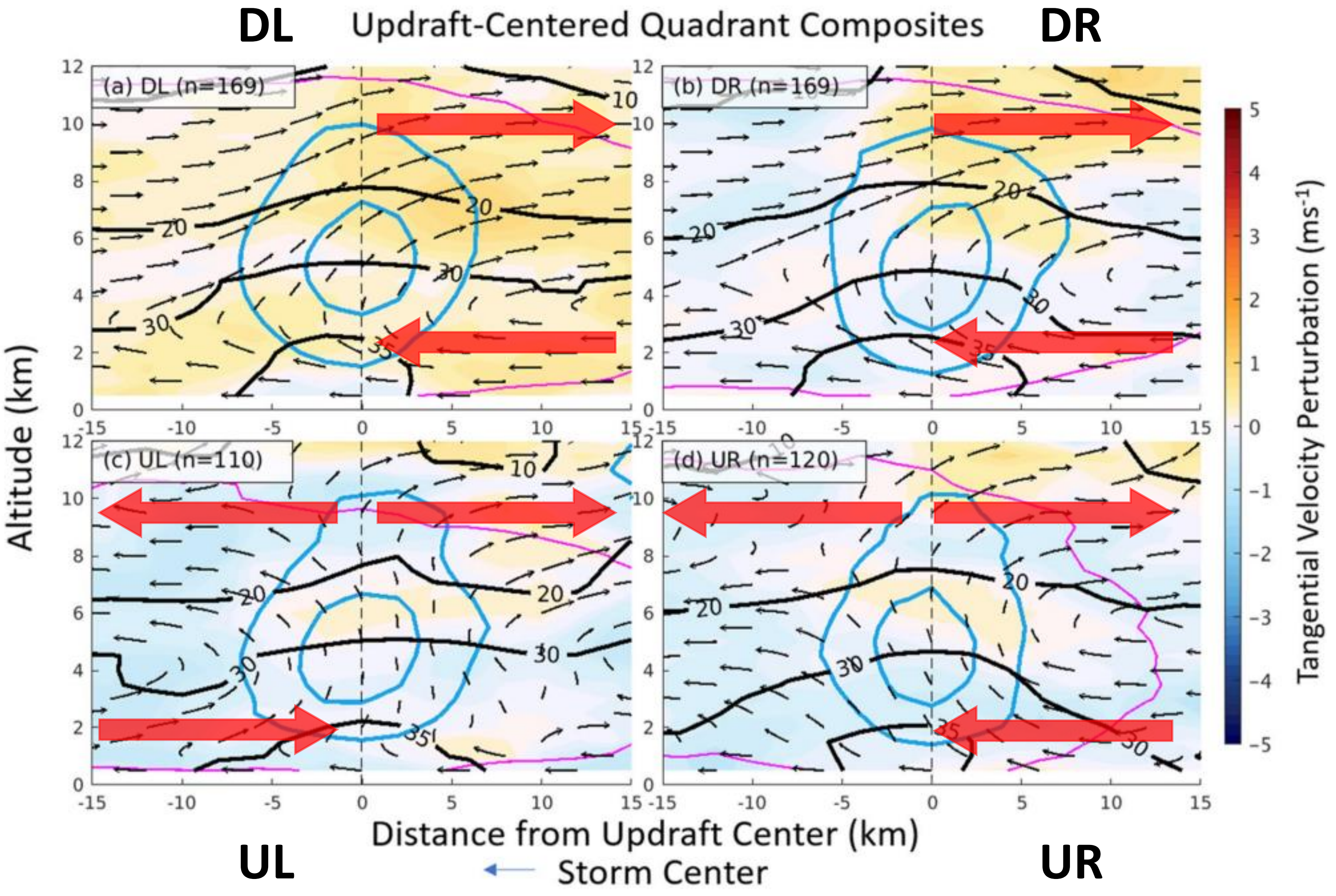

Total kinematics of updraft elements

Quadrant-averaged composites

Quadrant-averaged

- u and w (gray line)
- Reflectivity (black line)

Color: u

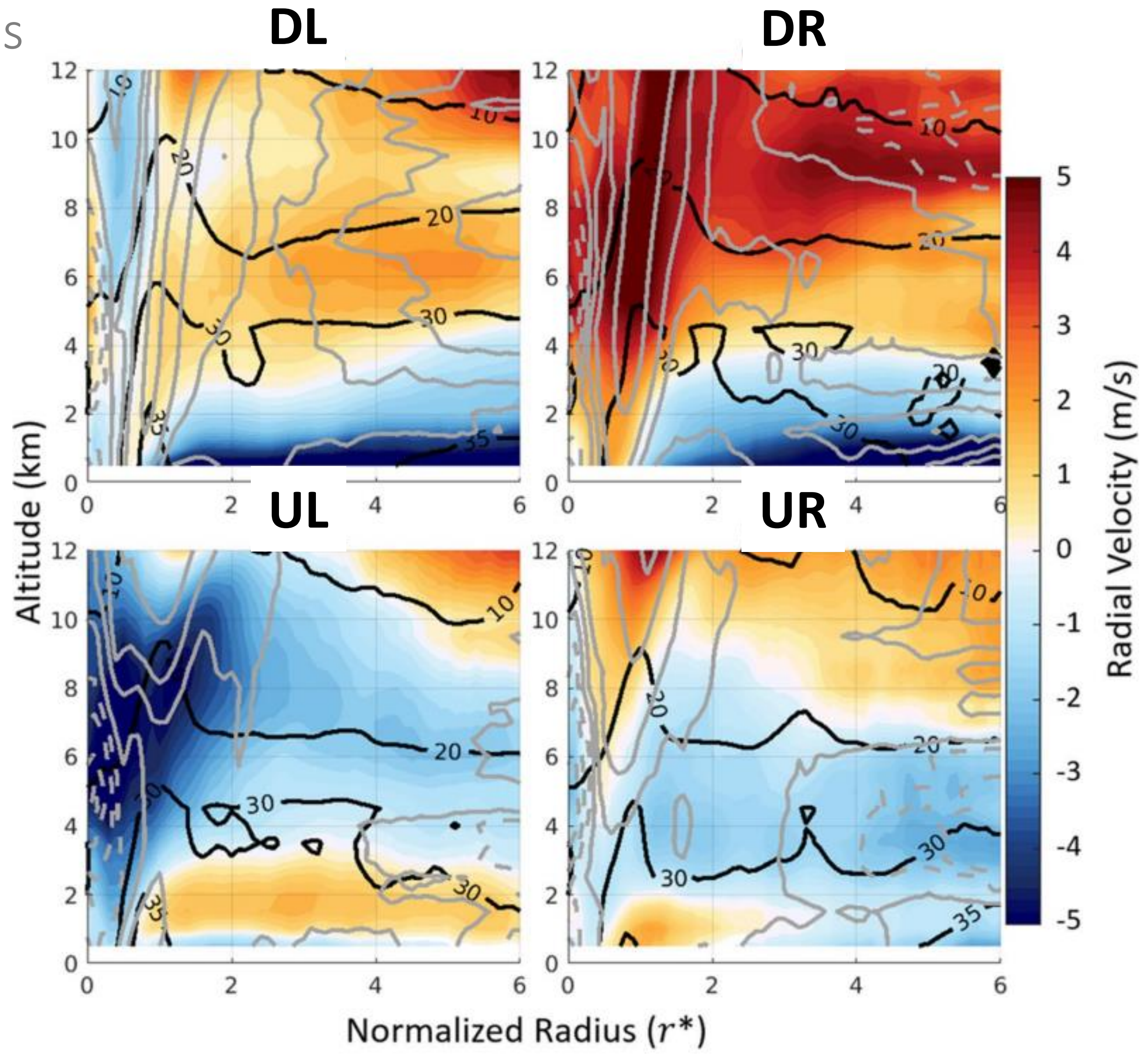

Total kinematics of updraft elements

Classification of Updraft Circulation Patterns

→ u and w

— Color: w

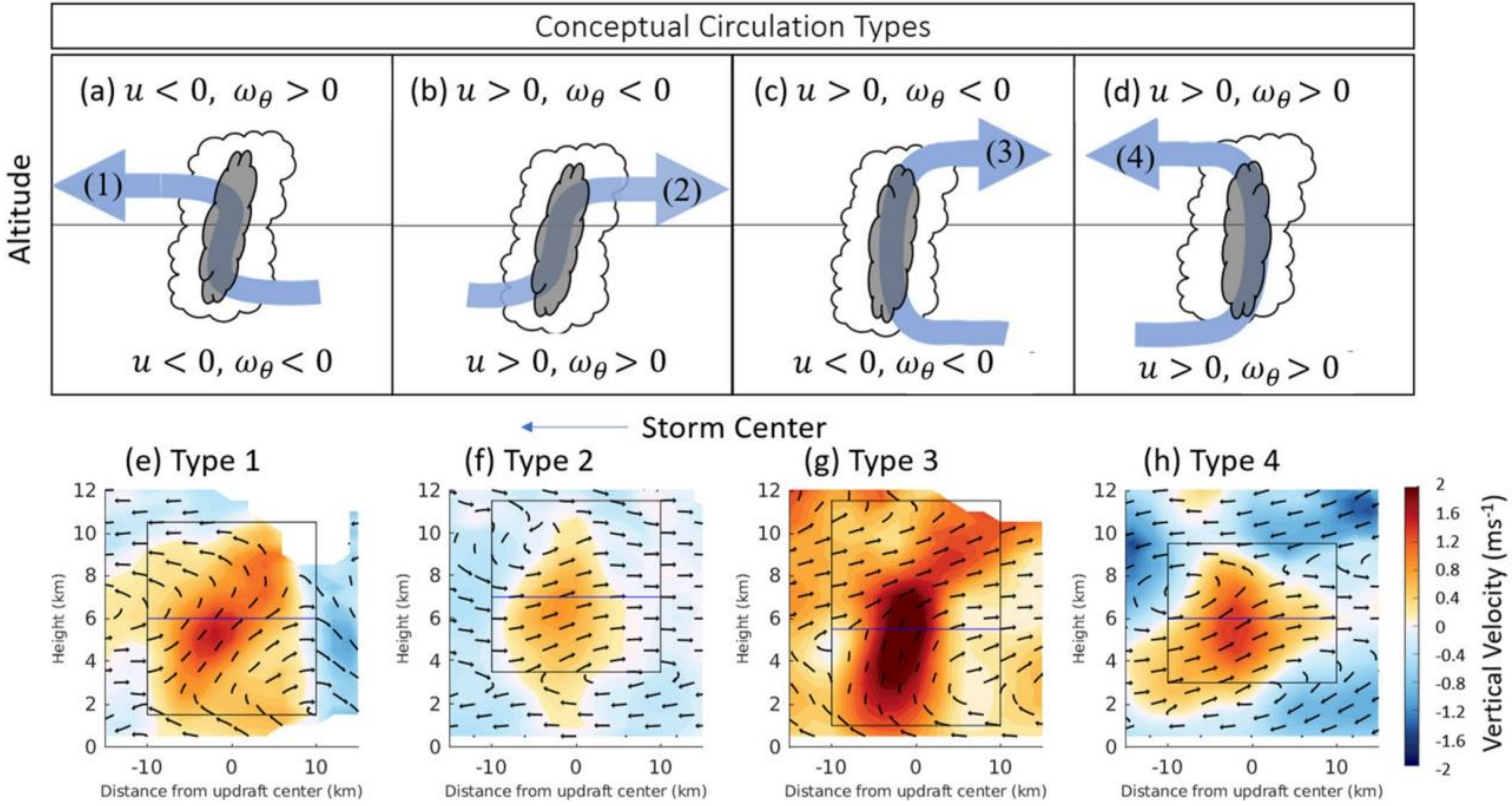

Total kinematics of updraft elements

Classification of Updraft Circulation Patterns

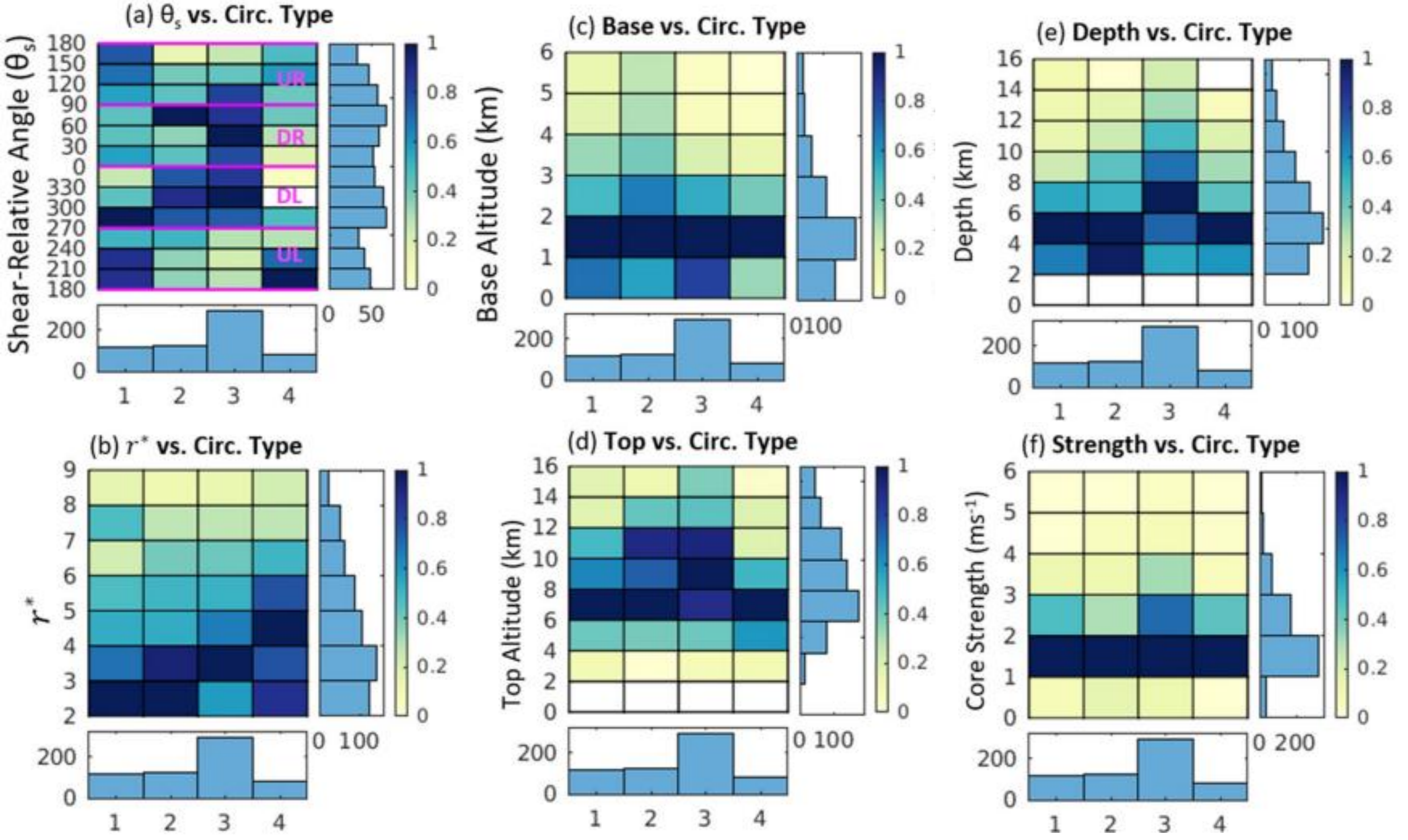

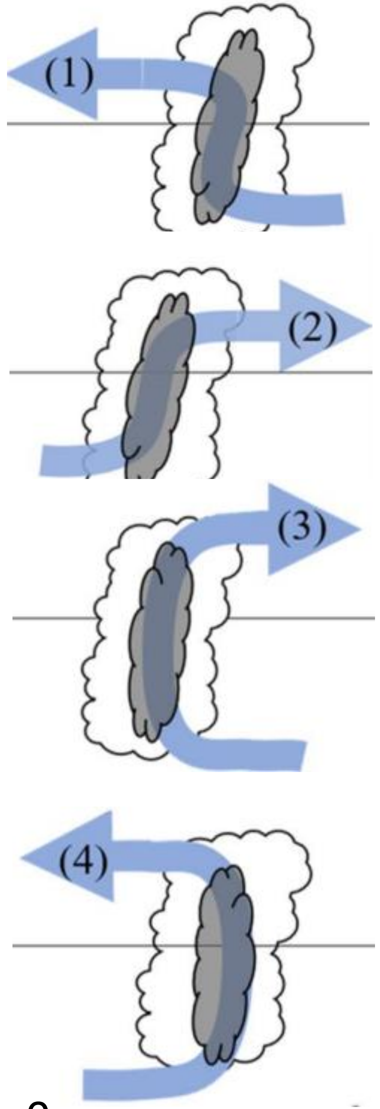

r = 0

Total kinematics of updraft elements

Azimuthal Variations in Updraft Size, Location, and Circulation Type

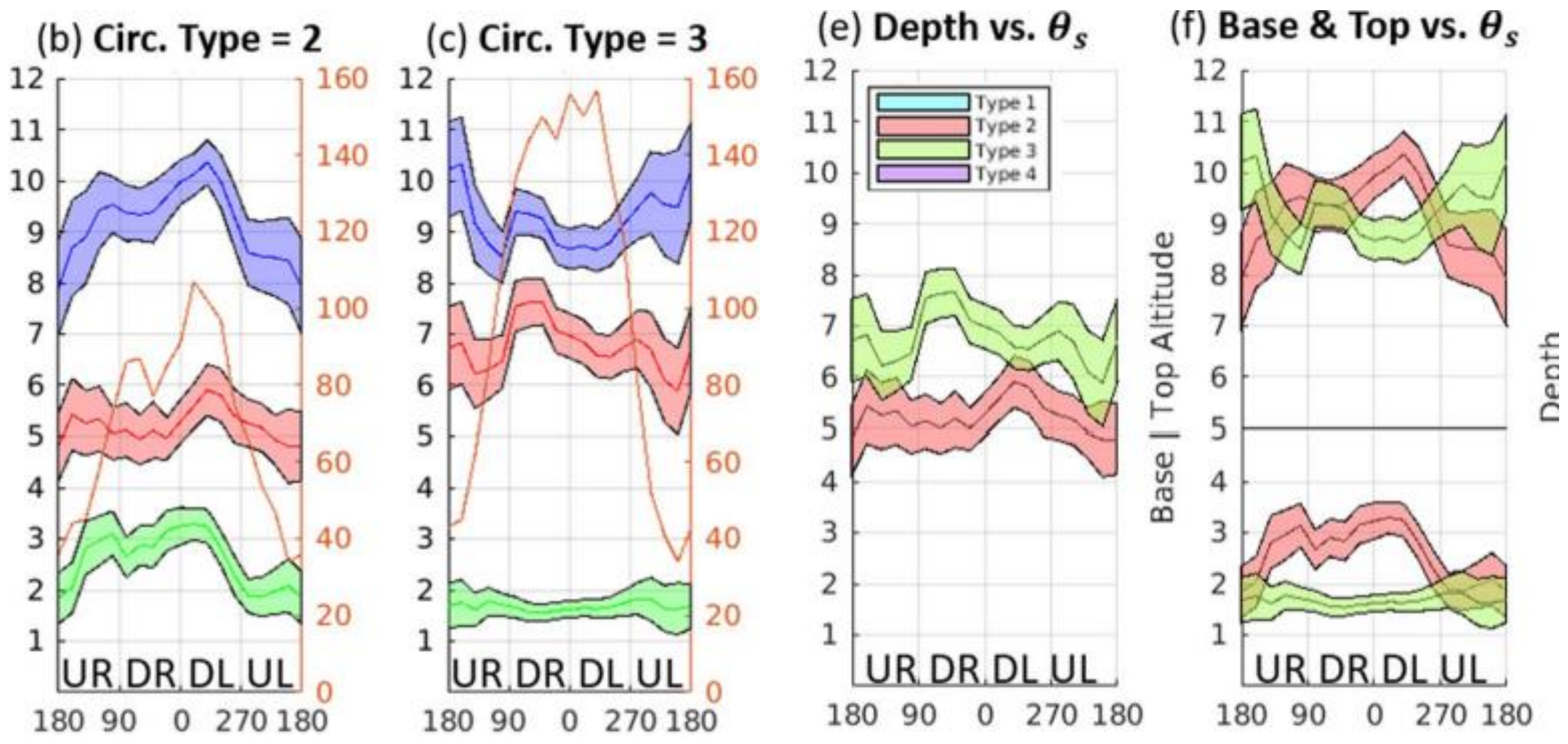

Total kinematics of updraft elements

Azimuthal Variations in Updraft Size, Location, and Circulation Type

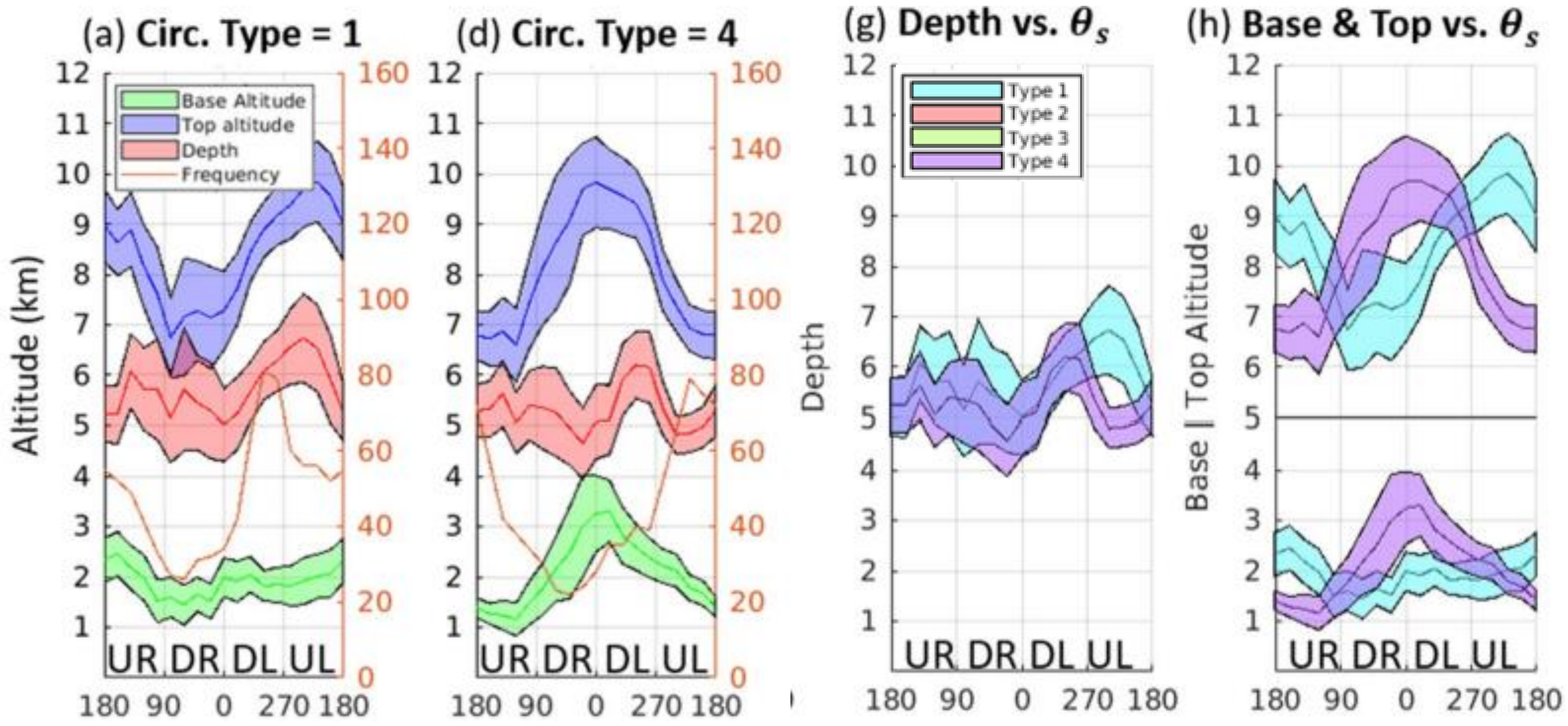

Discussions

- The upper-level radial flow try to match the wind shear vector. Convections with upper-level inflow (type 1 and 4) appear frequently at the upshear side, and those with upper-level outflow (type 2 and 3) appear frequently at the downshear side.
- At downshear side, the low-level inflow of convections (type 3) matched the low-level inflow layer in the storm-centered composites. The low-level outflow of convections (type2) matched the outflow above the low-level inflow.
- At upshear side, the low-level outflow of convections (type 4) matched the supergradient outflow layer at z = 1 ~ 2.5 km. The low-level inflow of convections (type 1) may occur above the supergradient outflow layer.

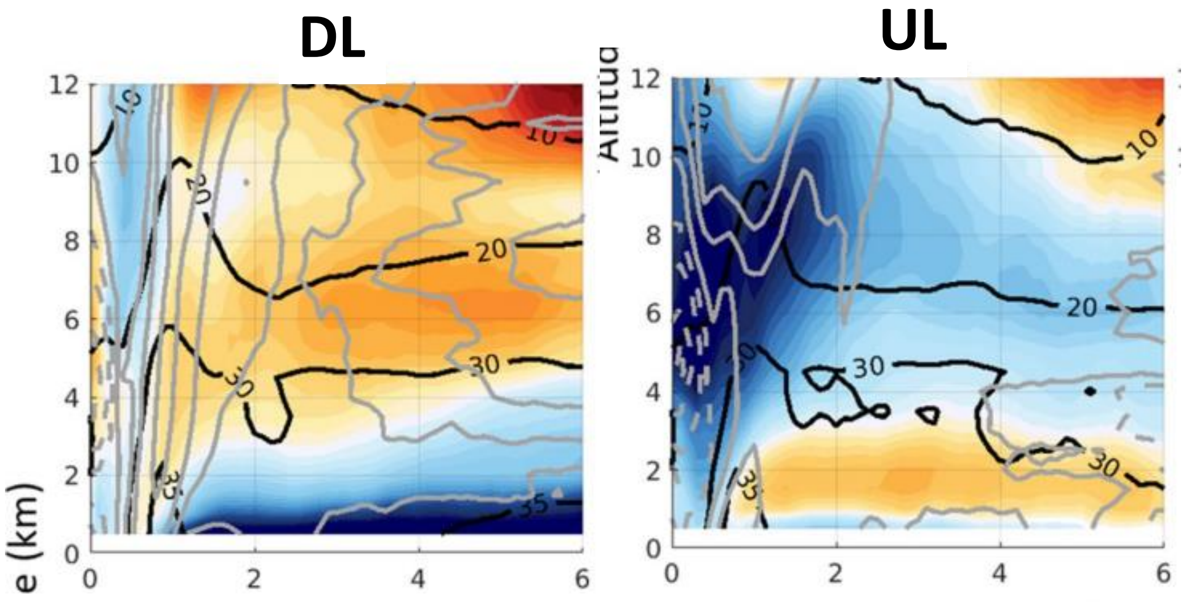

Total kinematics of updraft elements

Azimuthal Variations in Updraft Size, Location, and Circulation Type

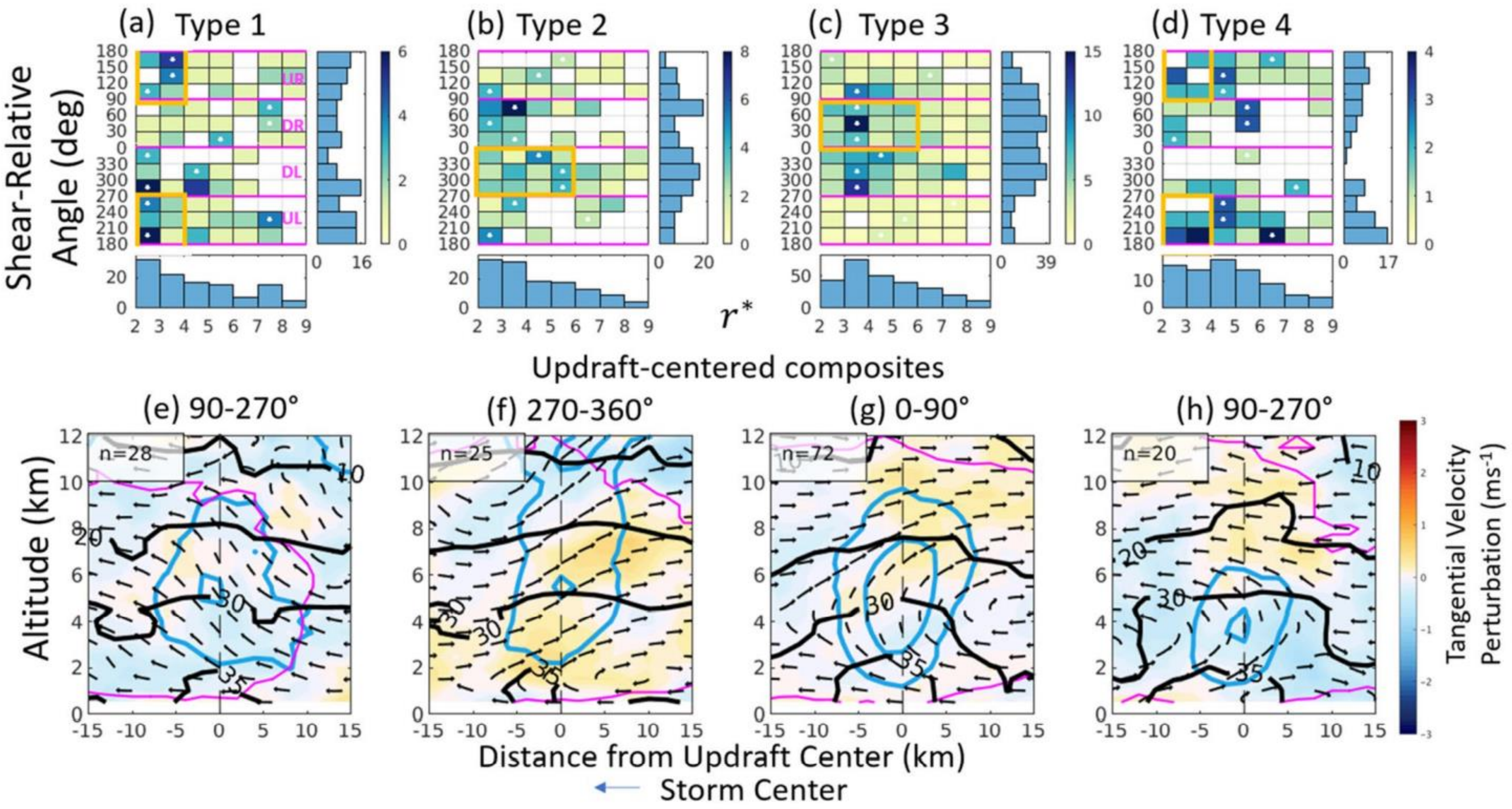

Total kinematics of updraft elements

Azimuthal Variations in Updraft Size, Location, and Circulation Type

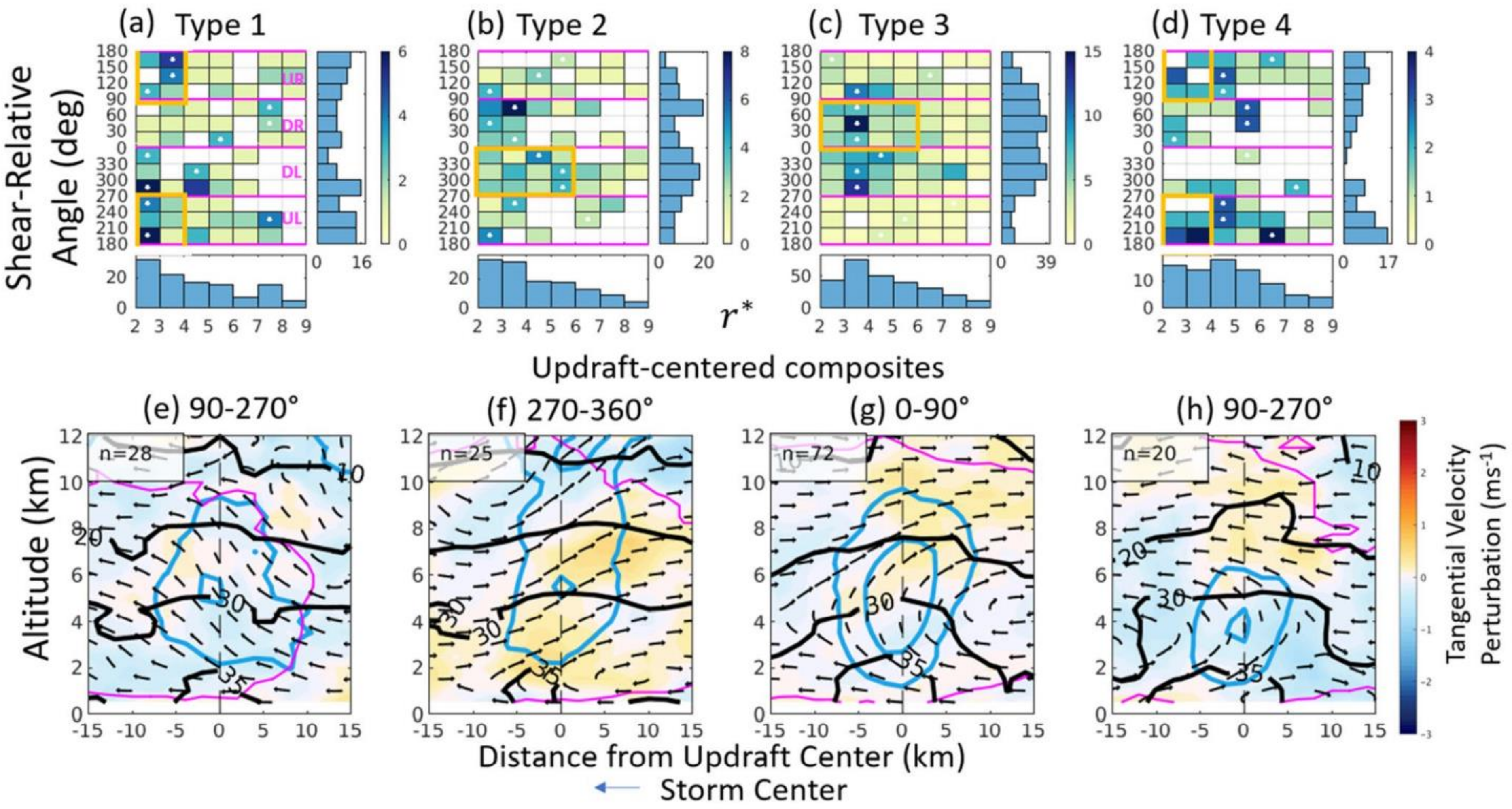

Conclusions

- This study examine rainband convective updrafts' kinematic and reflectivity characteristics observed by airborne Doppler radar across 2010-2019.
- Rainband updrafts become deeper and stronger with increasing radius due to increasing CAPE with radius.
- Rainband updradts are more (less) frequent and deeper (shallower) in the downshear (upshear) quadrants.
- The radial flow at the updraft base and top are dominated by vortex-scale and shear-induced background flow:
    1. Low-level inflow (outflow) and mid-level outflow (inflow) at the downshear (upshear) quadrant
    2. Decreasing depth in low-level inflow from DR to DL

Conclusions

- **DR**: It contains out-up-in flow, which is most frequent, deepest, and strongest along other types of updrafts.
- **DL**: Outflows exist above the updrafts. The reflectivity has convective features.
- **UL**: Inflow exist above the updrafts. Updraft bases connect with inflow or outflow at different height.
- **UR**: The radial flows vary largely at the base and top of the updrafts.

Shading: Reflectivity